Charge Disproportionation in Sr0.5Bi0.5FeO3 Containing Unusually High Valence Fe3.5+

Charge Disproportionation in Sr0.5Bi0.5FeO3 Containing Unusually High Valence Fe3.5+

Peng Xiong,[1] Fabio Denis Romero,[1,2] Yoshiteru Hosakai,[1] Haichuan Guo,[1] Takashi Saito,[1] We-Tin Chen,[3] Yu-Chun Chuang,[4] Hwo-Shuenn Sheu,[4] Graham McNally,[5] J. Paul Attfield,[5] and Yuichi Shimakawa[1,6]

[1]*Institute for Chemical Research, Kyoto University, Uji, Kyoto 611-0011, Japan*

[2]*Hakubi Project, Kyoto University, Yoshida-honmachi, Sakyo-ku, Kyoto 606-8501, Japan*

[3]*Center for Condensed Matter Sciences , National Taiwan University, No. 1, Sec. 4, Roosevelt Road, Taipei 10617, Taiwan*

[4]*National Synchrotron Radiation Research Center, 101 Hsin-Ann Road, Hsinchu Science Park, Hsinchu 30076, Taiwan*

[5]*Centre for Science at Extreme Conditions and School of Chemistry, The University of Edinburgh, Edinburgh EH9 3JZ, UK*

[6]*Integrated Research Consortium on Chemical Sciences, Uji, Kyoto 611-0011, Japan*

ABSTRACT: A Sr analog of $Ca_{0.5}Bi_{0.5}FeO_3$, $Sr_{0.5}Bi_{0.5}FeO_3$, containing unusually high-valence $Fe^{3.5+}$ ions was synthesized by using a high-pressure technique. It relieves the electronic instability due to the unusually high valence of $Fe^{3.5+}$ by a single charge disproportionation (CD) transition ($Fe^{3.5+} \rightarrow 0.75Fe^{3+} + 0.25Fe^{5+}$) rather than the successive CD and intersite charge transfer (CT) transitions seen in $Ca_{0.5}Bi_{0.5}FeO_3$. Conduction-band narrowing due to the significant bend in the Fe-O-Fe bond in the rhombohedral *R*–3*c* crystal structure stabilized the charge-disproportionated state at low temperatures. Most importantly, Bi^{3+} ions in $Sr_{0.5}Bi_{0.5}FeO_3$ do not act as counter cations accepting oxygen holes as they do in $Ca_{0.5}Bi_{0.5}FeO_3$, resulting in the absence of the intersite CT transition. The large cavity of the A-site Sr ions prevents the charge transferred Bi^{5+} from being stabilized. In the charge-disproportionated state the nearest-neighbor Fe^{3+} spins align antiferromagnetically and one quarter of the Fe^{3+} spins are randomly replaced by Fe^{5+} spins coupled ferromagnetically with the neighboring Fe^{3+} spins.

I. INTRODUCTION

Transition-metal ions with unusually high valence states can be stabilized in some oxides synthesized under strong oxidizing conditions.[1-5] Electronic instability due to such unusually high valence states is often relieved via charge transitions and these transitions are typically accompanied by drastic changes in structural, transport, and magnetic properties. Material systems containing unusually high valence ions thus provide excellent platforms for investigating complex charge-lattice-spin couplings.

Although the typical valence states of Fe ions in oxides are 2+ and 3+, unusually high valence states of Fe ions like Fe^{4+} can be stabilized in some oxides and are of particular interest. Fe^{4+} in the perovskite $CaFeO_3$, for instance, relieves its electronic instability by a very unusual charge change at 290 K: charge disproportionation (CD) to Fe^{3+} and Fe^{5+} ($2Fe^{4+} \rightarrow Fe^{3+} + Fe^{5+}$).[6] Because the strong hybridization of low-lying Fe-3d orbitals in Fe^{4+} with O-2p orbitals produces oxygen p holes (ligand holes, $\underline{L}$) in the electronic structure, the CD is expressed as localization of the ligand holes described as $2d^5\underline{L} \rightarrow d^5 + d^5\underline{L}^2$. The localization of the ligand holes at the Fe sites alternately makes a rock-salt type order of the $Fe^{3+}O_6$ and $Fe^{5+}O_6$ octahedra. Fe^{4+} in the cubic perovskite $SrFeO_3$, on the other hand, behaves differently. The itinerant ligand holes in $SrFeO_3$ are stabilized in the broad conduction bands due to the linear Fe-O-Fe bonds and are tolerant to delocalization.[9] As the result. $SrFeO_3$ stays metallic down to low temperatures and does not undergo a charge transition.

The perovskite $Ca_{0.5}Bi_{0.5}FeO_3$ can be obtained by substituting Bi^{3+} ions for half of the Ca^{2+} ions in $CaFeO_3$, and the doped electrons change the unusually high-valence Fe^{4+} to $Fe^{3.5+}$.[10] This electron doping induces charge behaviors different from the CD in $CaFeO_3$, and when cooled the compound shows successive transitions due to CD ($Ca_{0.5}Bi_{0.5}Fe^{3.5+}O_3 \rightarrow Ca_{0.5}Bi_{0.5}Fe^{3+}{}_{0.67}Fe^{4.5+}{}_{0.33}O_3$) at 250 K and inter intersite charge transfer (CT) between B-site Fe and A-site Bi ($0.25Bi^{3+} + 0.33Fe^{4.5+} \rightarrow 0.25Bi^{5+} + 0.33Fe^{3+}$) at 200 K. The Bi ions in $Ca_{0.5}Bi_{0.5}FeO_3$ are the counter cations accepting the charge transferred from the unusually high-valence Fe ions, as in the intersite CT in $BiNiO_3$ under pressure ($Bi^{3+}Ni^{3+}O_3 \rightarrow Bi^{3+}{}_{0.5}Bi^{5+}{}_{0.5}Ni^{2+}O_3$).[8] The CT transition occurring after the CD transition completely relieves the electronic instability of $Fe^{3.5+}$ in $Ca_{0.5}Bi_{0.5}FeO_3$. Both are accompanied by the changes in structural and magnetic properties, indication strong couplings of the charge, lattice and spin in $Ca_{0.5}Bi_{0.5}FeO_3$.

Our primary concern is what kind of charge transitions would be induced in Bi-doped $SrFeO_3$. Although Fe^{4+} in $SrFeO_3$ shows neither CD nor CT transitions, it is of interest how the instability of unusually high-valence $Fe^{3.5+}$ is relieved in the presence of Bi^{3+} that can be oxidized to Bi^{5+}. In this study we prepared the novel perovskite $Sr_{0.5}Bi_{0.5}FeO_3$ under a high-pressure and high-temperature condition and found that at low temperatures it shows a single CD transition of the $Fe^{3.5+}$ to Fe^{3+} and Fe^{5+} in a 3:1 ratio. The Bi ions in $Sr_{0.5}Bi_{0.5}FeO_3$, unlike those in $Ca_{0.5}Bi_{0.5}FeO_3$, did not induce an intersite CT transition. We investigated the compound's crystal and magnetic structures, and here

we discuss the observed CD transition.

II. EXPERIMENTAL

$Sr_{0.5}Bi_{0.5}FeO_3$ was prepared by a solid-state reaction under a high-pressure and high-temperature condition. Starting materials ($SrCO_3$, Bi_2O_3, and Fe_2O_3) were well mixed and calcined at 850°C. The resultant polycrystalline sample and oxidizing agent $KClO_4$ were well ground, sealed in a platinum capsule, treated at 6 GPa and 1200 °C for 30 minutes, and then quenched to room temperature before the pressure was released.

The crystal and magnetic structures of $Sr_{0.5}Bi_{0.5}FeO_3$ were analyzed by evaluating synchrotron X-ray powder diffraction (SXRD) and neutron powder diffraction (NPD) data. The SXRD data from room temperature to 80 K were collected with a wavelength of 0.82656 Å at the beamline TPS09A at the National Synchrotron Radiation Research Center. The sample was packed into a glass capillary with an inner diameter of 0.1 mm. The obtained data was analyzed by the Rietveld method using the RIETAN-FP program. [11] NPD measurements were performed on a sample contained in a vanadium can using the WISH diffractometer at the ISIS neutron source, Rutherford Appleton Laboratory, UK. The diffraction data were analyzed with the GSAS suite programs.[12]

To investigate the valence and magnetic states of Fe ions in $Sr_{0.5}Bi_{0.5}FeO_3$, ^{57}Fe Mössbauer spectroscopy measurements were carried out in a transmission geometry with a constant-acceleration spectrometer by using a $^{57}Co/Rh$ radiation source. α-Fe was used to calibrate the velocity scale, the isomer shift (IS) and the hyperfine field (HF). The obtained spectra were fitted to Lorentzian functions by using the standard least-squares method.

Magnetic properties of the sample were measured with a SQUID magnetometer (MPMS Quantum Design). Resistivity was measured with a standard four-probe method by using a commercial Physical Property Measurement system (Quantum Design).

III. RESULTS AND DISCUSSION

The obtained sample was a nearly single phase (unreacted Fe_2O_3 <1%). Room temperature SXRD peaks could be indexed with a rhombohedral *R*–3*c* unit cell in the space group (No. 167). Crystal structure was analyzed by the Rietveld method with SXRD and NPD data, and the results are shown in Figures 1a and 1b. The structure parameters obtained from the analysis are listed in Table I. The rhombohedral crystal structure is slightly distorted from the cubic perovskite. The refined occupancies for the A-site Sr/Bi were respectively 0.486/0.514(3), indicating random distribution of the ions at the site. The oxygen site occupancy refined with the NPD data was 0.991(2), indicating the oxygen stoichiometry of the compound. The occupancy for oxygen was fixed to 1 in the final refinement.

Given the composition of $Sr_{0.5}Bi_{0.5}FeO_3$ with typical-valence Sr^{2+}, Bi^{3+}, and O^{2-} ions, unusually high-valence $Fe^{3.5+}$ is suggested in this compound. The bond valence sum (BVS)[13, 14] value calculated from the Fe-O bond lengths obtained from the structure refinement results is 3.4+, in

consistence with the nominal valence state of Fe. The unusually high valence state of Fe was also confirmed by Mössbauer spectroscopy, as shown in Figure 2. The spectrum at room temperature consists of a singlet with an IS of 0.20 mm/s, which is between the typical values for Fe^{3+} (≈ 0.54 mm/s)[15] and Fe^{4+} (≈ 0.07 mm/s)[6] for octahedral oxygen coordination and is also very close to the value for $Fe^{3.5+}$ observed in $Ca_{0.5}Bi_{0.5}FeO_3$.

The present $Sr_{0.5}Bi_{0.5}FeO_3$ containing unusually high-valence $Fe^{3.5+}$ is thus a Sr analog of the previously reported $Ca_{0.5}Bi_{0.5}FeO_3$. The compound can also be considered to be Bi^{3+}-doped $SrFeO_3$, where the doped electrons due to the substitution of Bi^{3+} for Sr^{2+} produces $Fe^{3.5+}$ at the B-site. The substitution also causes rhombohedral structural distortion with a significant bend (165.5(2)°) in the Fe-O-Fe bond from the 180° bonding in cubic $SrFeO_3$. Note that the Fe-O-Fe bond angle is larger than that in orthorhombic $Ca_{0.5}Bi_{0.5}FeO_3$ (155.3°).

On cooling the sample, no apparent structural phase transitions were observed. Temperature dependences of the lattice parameters and the cell volume, plotted in Figure 3, show monotonic decrease down to about 80 K. The observed behavior is in sharp contrast to that due to the successive structural phase transitions caused by the CD at 250 K and CT at 200 K in $Ca_{0.5}Bi_{0.5}FeO_3$.

Although no structural transition was observed, an unusual charge change occurred in the present $Sr_{0.5}Bi_{0.5}FeO_3$. The Mössbauer spectrum taken at 4 K (Figure 2) clearly shows a charge-disproportionated state of Fe. The spectrum consists of two sextets, with ISs of 0.43 and 0.00 mm/s, in a 3:1 ratio. These sextets are very similar to those observed in the charge-disproportionated state of $CaFeO_3$ and are assigned to Fe^{3+} and Fe^{5+}. The Mössbauer results therefor reveal that the CD transition $Fe^{3.5+} \rightarrow 0.75Fe^{3+} + 0.25Fe^{5+}$ takes place at a low temperature in $Sr_{0.5}Bi_{0.5}FeO_3$. Although the charge-disproportionated state in $Sr_{0.5}Bi_{0.5}FeO_3$ is evident, the transition temperature is difficult to determine. When we examine the temperature dependence of electrical resistivity (Figure 4) in detail, however, we see that below 230 K it deviates from the normal semiconductor behavior. In the temperature dependence of magnetic susceptibility (Figure 5b) an anomaly at about 230 K is seen. The Mössbauer spectrum taken at 200 K looks a single peak, but is much broader than the room temperature one and actually can be fitted with 3:1 components of paramagnetic Fe^{3+} and Fe^{5+} (Figure S2 and Table SII). Because no other anomalies were observed in temperature-dependent experimental data, he CD transition temperature of $Sr_{0.5}Bi_{0.5}FeO_3$ appears to be around 230 K. The absence of significant changes in the unit cell volume at the CD transition temperature is similar to the transition behaviors observed in $CaFeO_3$ [1] and $La_{1/3}Sr_{2/3}FeO_3$.[16]

It is interesting to note that the Bi^{3+} substitution does not induce a CT transition in $SrFeO_3$, which stays metallic down to low temperatures without any charge transition, whereas it induces a CT transition in $CaFeO_3$, which originally shows a CD transition. Unlike the Bi ions in $Ca_{0.5}Bi_{0.5}FeO_3$, the Bi ions in $Sr_{0.5}Bi_{0.5}FeO_3$ cannot be counter cations accepting the oxygen holes from the unusually high-valence Fe ions, resulting in the absence of a CT transition. The Bi^{3+} substitution causes the conduction-band narrowing, at low temperature, due to the significant bend (165.5 (2) °) in the Fe-O-Fe bond from the 180° bonding in $SrFeO_3$. Therefore the ligand holes of $Fe^{3.5+}$ are localized at some of the Fe sites making the $d^5\underline{L}^2$ electronic state but not at the Bi sites. A negative chemical pressure applied to the Bi^{3+} ions (ionic radius = 1.03 Å for 6 oxygen coordination[17]) by the large cavity of the A-site Sr^{2+} ions (1.18 Å) prevents the much smaller Bi^{5+} ions (0.76 Å) from being stabilized,

suppressing the intersite CT transition. In this sense, the situation is rather similar to the CD transition in $La_{0.5}Sr_{0.5}FeO_3$.[18] Although the Mössbauer spectrum of $Sr_{0.5}La_{0.5}FeO_3$ at low temperature was analyzed with three components, their IS values suggest the essential 3:1 CD of Fe^{3+} and Fe^{5+}. The Fe-O-Fe bond angle in $Sr_{0.5}Bi_{0.5}FeO_3$ (165.5(2)°) is also to that in $Sr_{0.5}La_{0.5}FeO_3$ (167.8(2)°). (The crystallographic data of our $Sr_{0.5}La_{0.5}FeO_3$ sample is listed in the Supporting information Table S1.) Like La^{3+} in $Sr_{0.5}La_{0.5}FeO_3$, Bi^{3+} in $Sr_{0.5}Bi_{0.5}FeO_3$ does not trigger a CT transition relieving the electronic instability of $Fe^{3.5+}$.

In the charge-disproportionated state at low ow temperature there is no indication of ordering of the 3:1 Fe^{3+} and Fe^{5+} ions in either the SXRD or NPD patterns. In the low-temperature (5 K) NPD pattern, however, magnetic superstructure reflections are evidently included. The magnetic order of the Fe spins in the CD state is consistent with the Mössbauer spectroscopy measurement result at 4 K, where both Fe^{3+} and Fe^{5+} components consist of sextets with large HFs. Assuming that the magnetic moments of all Fe ions are the same due to the random distribution of the Fe^{3+} and Fe^{5+} ions, the observed magnetic reflections are reproduced well with a G-type antiferromagnetic structure of the B-site Fe spins and the magnetic structure analysis gives the refined magnetic moment of 2.01(1) μ_B. The refined profile of low-temperature NPD is plotted in Figure 1c and the refined structure parameters are listed in Table S2.

The proposed magnetic structure is shown in Figure 6. In the G-type antiferromagnetic structure, where the nearest-neighbor spins align in an antiparallel way, one quarter of the Fe^{3+} spin sites are randomly replaced by Fe^{5+} spins. According to the Kanamori-Goodenough rules, those Fe^{5+} spins couple ferromagnetically with the neighboring Fe^{3+} spins, and that is why the refined G-type antiferromagnetic moment is significantly reduced. Although this spin arrangement gives 8 μ_B per 4 Fe spins, those hypothetical ferromagnetic moments cancel out and no net magnetization would be produced due to the random distribution of the Fe^{5+} spins. This magnetic structure model is also consistent with the linear behavior observed in the isothermal *M-H* measurements below the CD transition temperatures (Figure 5c). The small refined magnetic moments at Fe spin sites may indicate another magnetic structure model with Fe^{5+} spin moments oriented random directions, as they have been proposed to be oriented in $CeCu_3Fe_4O_{12}$, which also contains $Fe^{3.5+}$ at B-site in the A-site-ordered perovskite structure and shows a similar 3:1 CD of Fe^{3+} and Fe^{5+}.[19] However, the present magnetic property measurement results do not support that model because neither net magnetization in the *M-H* measurements nor peak broadening of the Fe^{5+} Mössbauer spectrum below the CD transition temperature was observed.

The magnetic transition temperature due to charge-disproportionated Fe^{3+} and Fe^{5+} spins was difficult to determine from the magnetic susceptibility measurement (Figure 4a). Nonetheless, the observed susceptibility blow about 150 K shows large hysteresis between the field-cooled (FC) and zero-field-cooled (ZFC) mode measurements. The Mössbauer spectrum taken at 150 K apparently contains magnetically ordered sextet components (Figure S2). Therefore the antiferromagnetic transition temperature of $Sr_{0.5}Bi_{0.5}FeO_3$ appears to be about 150 K, which is lower than the CD transition temperature. The behavior that the magnetic ordering of Fe^{3+} and Fe^{5+} spins occurs and is followed by the CD transition is similar to the behaviors observed in $CaFeO_3$ and Ca_2FeMnO_6 [20] and is different from the simultaneous charge and spin transitions in $CaCu_3Fe_4O_{12}$.[21]

The behavior is also very different from the successive charge transitions in $Ca_{0.5}Bi_{0.5}FeO_3$ with an idle spin state between the CD and intersite CT transition temperature.[22]

IV. SUMMARY

The novel compound $Sr_{0.5}Bi_{0.5}FeO_3$, containing unusually high-valence $Fe^{3.5+}$ ions, was synthesized under a high-pressure and high-temperature condition. Rietveld refinements of SXRD and NPD data confirmed that the compound crystallized in a distorted perovskite structure with the rhombohedral space group $R\bar{3}c$. Mössbauer spectroscopy study revealed that CD ($Fe^{3.5+} \rightarrow 0.75Fe^{3+} + 0.25Fe^{5+}$) took place below 230 K. The charge-disproportionated Fe^{3+} and Fe^{5+} spins magnetically order at about 150 K, which is below the CD transition temperature. The magnetic structure was solved by a combined analysis of low-temperature NPD profile and isothermal magnetization data. The nearest-neighbor Fe^{3+} spins align antiferromagnetically, giving the G-type antiferromagnetic structure and one quarter of the Fe^{3+} spin sites are randomly replaced by Fe^{5+} spins coupled ferromagnetically with the neighboring Fe^{3+} spins. The random distribution of the Fe^{5+} spins is consistent with the linear behavior evident in the *M-H* measurements.

Unlike $Ca_{0.5}Bi_{0.5}FeO_3$, which shows successive CD and intersite CT transitions, the Sr analog $Sr_{0.5}Bi_{0.5}FeO_3$ shows a single CD transition ($Fe^{3.5+} \rightarrow 0.75Fe^{3+} + 0.25Fe^{5+}$) relieving the electronic instability due to the unusually high valence of $Fe^{3.5+}$. A significant bend in the Fe-O-Fe bond in the rhombohedral $R\bar{3}c$ crystal structure makes the conduction bands narrow, stabilizing the charge-disproportionated state at low temperatures. The Bi^{3+} ions in $Sr_{0.5}Bi_{0.5}FeO_3$ cannot be counter cations accepting oxygen holes as they do in $Ca_{0.5}Bi_{0.5}FeO_3$, resulting in the absence of an intersite CT transition. A negative chemical pressure applied to the Bi^{3+} ions by the large cavity of the A-site Sr^{2+} ions prevents the much smaller Bi^{5+} ions from being stabilized, suppressing the intersite CT transition.

References

[1] Y. Takeda, S. Naka, M. Takano, T. Shinjo, T. *et al*, *Mater*. *Res*. *Bull*. 1978, 13, 61– 66.

[2] P. K. Gallagher, J. B. MacChesney, D. N. E. Buchanan, *J*. *Chem*. *Phys*. 1964, 41, 2429-2434.

[3] G. Demazeau, A. Marbeuf, M. Pouchard, *et al*., *J*. *Solid Chem*. 1971, 3(4), 582-589.

[4] G. Demazeau, C. Parent, M. Pouchard, P. Hagenmuller, *Mater*. *Res*. *Bull*. 1972, 7, 913-920.

[5] S. Ishiwata, M. Azuma, M. Takano, *et al*., *J*. *Mater*. *Chem*. 2002, 12, 3733-3737.

[6] M. Takano, N. Nakanishi, Y. Takeda, S. Naka, T. Takada, *Mater*. *Res. Bull*. 1977, 12, 923–928.

[7] J. B. Torrance, P. Lacorre, A. I. Nazzal, *et al*., *Phys*. *Rev*. B. 1992, 45, 8209-8212.

[8] M. Azuma, S. Carlsson, J. Rodgers, et al., *J*. *Am*. *Chem*. *Soc*. 2007, 129, 14433-14436.

[9] T. Takeda, Y. Yamaguchi, H. Watanabe, *J*. *Phys*. *Soc*. *Jpn*. 1972, 33, 967-969.

[10] Y. Hosaka, F. D. Romero, N. Ichikawa, *et al*., *Angew*. *Chem*. Int. Ed., 2017, 56, 4243-4246.

[11] F. Izumi, K. Momma, *Solid state Phenom*. 2007, 130, 15-20.

[12] B. Toby, *J*. *Appl*. *crystallogr*. 2001, 34. 210-213.

[13] I. D. Brown. *Chem*. *Soc*. *Rev*. 1978, 7, 359-376.

[14] I. D. Brown, D. Altermatt, *Acta Crystallogr*., Sect. B: Struct. Sci. 1985, 41, 244-247.

[15] M. Eibschütz, S. Shtrikman, D. Treves, *Phys*. *Rev*. B. 1967, 156, 562-577.

[16] P.D. Battle, T. C. Gibb and P. Lightfoot. *J*. *Solid State Chem*. 1989, 84,271-279.

[17] R. D. Shannon. *Acta Cryst*. 1976, A32, 751-767. Because no reliable ionic radius for Bi^{3+} for 12 oxygen coordination was reported, we tentatively use the ionic radii for 6 oxygen corrdination.

[18] M. Takano, J. Kawachi, N. Nakanishi, *et al*., *J*. *Solid State Chem*., 1981, 39, 75-84.

[19] I.Yamada, H. Etani, M. Murakami, *et al*., *Inorg*. *Chem*. 2014, 53, 11794-11801.

[20] Y. Hosaka, N. Ichikawa, T. Saito, *et al*., *J*. *Am*. *Chem*. *Soc*., 2015, 137, 7468-7473.

[21] I. Yamada, M. Murakami, N. Hayashi, *et al*., *Inorg*. *Chem*. 2015, 55, 1715-1719.

[22] F. D. Romero, Y. Hosaka, N. Ichikawa, *et al*., *Phys*. *Rev*. B, 2017, 96, 064434.

Figures

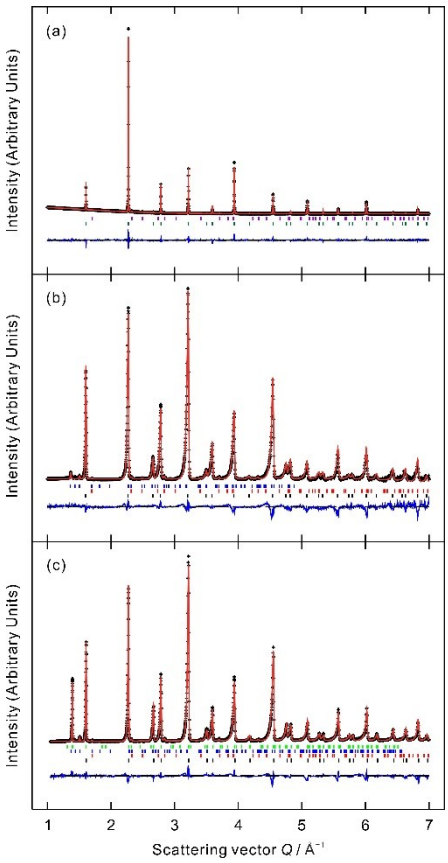

Figure1. Rietveld refinement profiles for $Sr_{0.5}Bi_{0.5}FeO_3$. (a) Room-temperature SXRD data. The top and bottom vertical bars respectively indicate the diffraction peak positions for $Sr_{0.5}Bi_{0.5}FeO_3$ and impurity Fe_2O_3. (b) Room-temperature ND data. The top bars indicate the nuclear diffraction of $Sr_{0.5}Bi_{0.5}FeO_3$. The middle and bottom bars respectively show the nuclear and magnetic reflection of impurity Fe_2O_3. (c) ND data collected at 4 K. The top and second vertical bars respectively show the nuclear and magnetic reflections of $Sr_{0.5}Bi_{0.5}FeO_3$. The third and bottom vertical bars respectively show the nuclear and magnetic reflections of impurity Fe_2O_3.

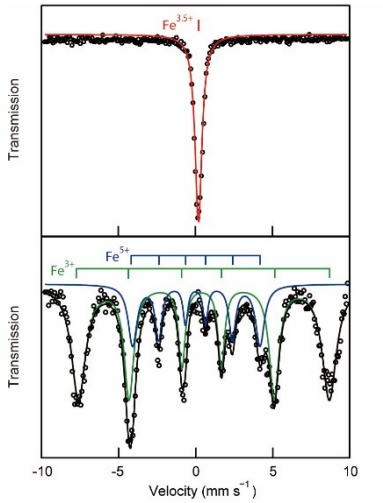

Figure 2. Mössbauer spectrum of $Sr_{0.5}Bi_{0.5}FeO_3$ at room temperature (top panel) and 4 K (bottom panel). The black circles show experimental data and the solid lines show the fittings.

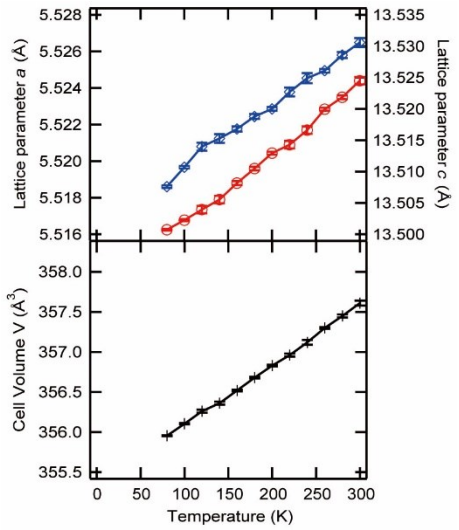

Figure 3. Temperature dependence of the lattice parameters *a* and *c* which is which?and cell volume V of $Sr_{0.5}Bi_{0.5}FeO_3$ in hexagonal rhombohedral *R*−3*c* lattice.

Comment – we might get useful information from lattice strains. Try plotting a and $c/\sqrt{6}$ on the same scale, and also plot the strain $(a- c/\sqrt{6})/a$ to see if this shows the transitions

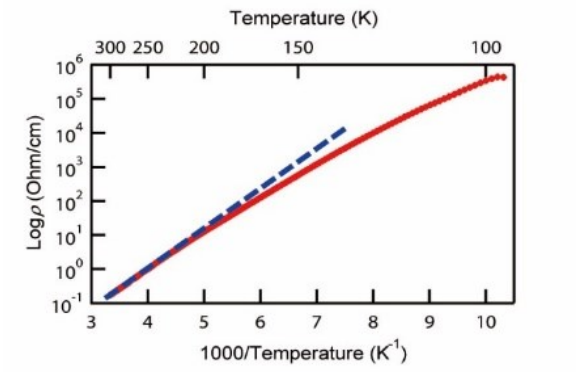

Figure 4. Temperature dependence of the electrical resistivity as a plot of logρ versus 1000/T. The blue dashed line represents a typical semiconductor change given by an Arrhenius equation.

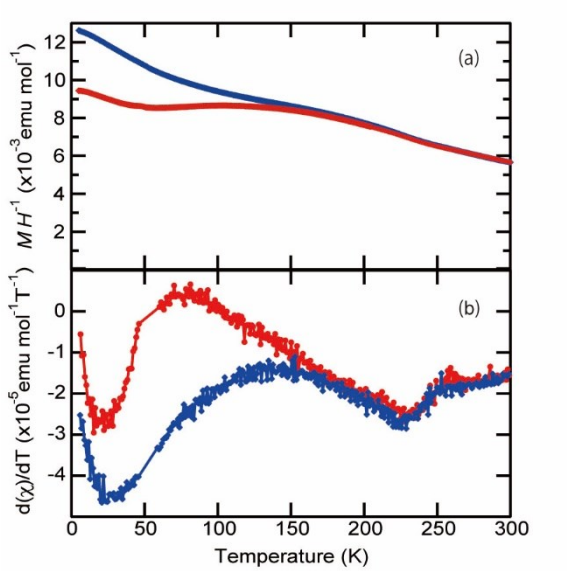

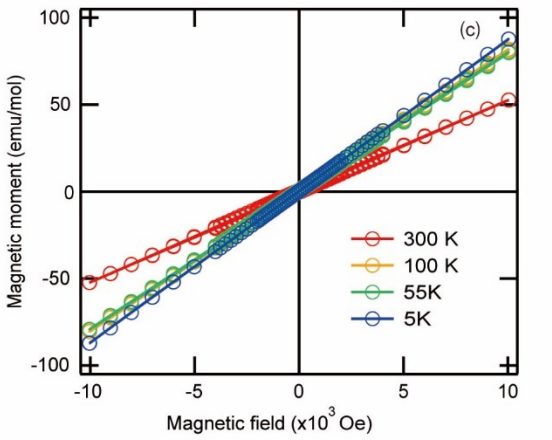

Figure 5. (a) Temperature dependence of the magnetic susceptibility of $Sr_{0.5}Bi_{0.5}FeO_3$ in a 10 kOe external magnetic field. The red and blue curves respectively represent ZFC and FC susceptibility. (b) Differential plots of the magnetic susceptibility data. (c) Isothermal magnetization curves measured at temperatures between 300 K and 5 K.

comment – we should plot the average G type magnetic structure somewhere also

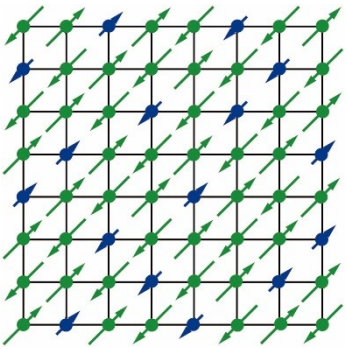

Figure 6. Schematic drawing of the proposed magnetic structure of $Sr_{0.5}Bi_{0.5}FeO_3$. The green and blue arrows respectively represent spins of charge-disproportionated Fe^{3+} and Fe^{5+}.

TABLES

Table I. Refined structural parameters of $Sr_{0.5}Bi_{0.5}FeO_3$ at room temperature.
In the structure refinement the rhombohedral crystal structure was analyzed with the hexagonal cell. The BVS results calculated from the cation-O bond lengths are also listed. uiso units

Atom	Site	*x*	*y*	*z*	U_{iso}	Occupancy	BVS
Sr	6*a*	0	0	0.25	0.028 (4)	0.486(3)	2.3
Bi	6*a*	0	0	0.25	0.028(4)	0.514(-)	2.2
Fe	6*b*	0	0	0	0.0037(4)	1.0	3.4
O	18*e*	0.5446(6)	0	0.25	0.0013(8)	1.0	-

Space group: *R*–3*c*. *a* = 5.5243 (2) Å, *c* = 13.5306 (7) Å, and R_{wp} = 2.7%.

Table II. Mössbauer parameters for $Sr_{0.5}Bi_{0.5}FeO_3$ at room temperature and 4 K.

Temperature	Components	IS (mm/s)	HF (kOe)	Area Ratio (%)

Room temperature	$Fe^{3.5+}$	0.23	0.00	100
4 K	Fe^{3+}	0.43	50.4	75.1
	Fe^{5+}	0.00	25.6	24.9

Supplemental Information

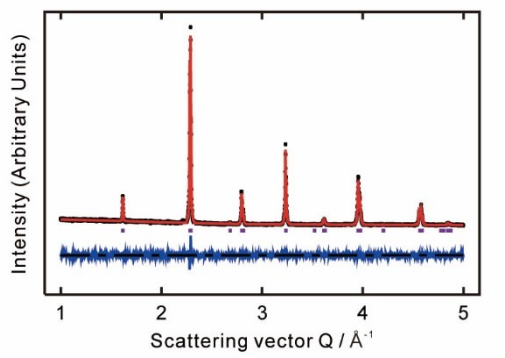

Figure. S1 Refinement profiles for $Sr_{0.5}La_{0.5}FeO_3$ against room temperature XRD data. The purple vertical bars indicate the diffraction peak positions for $Sr_{0.5}La_{0.5}FeO_3$.

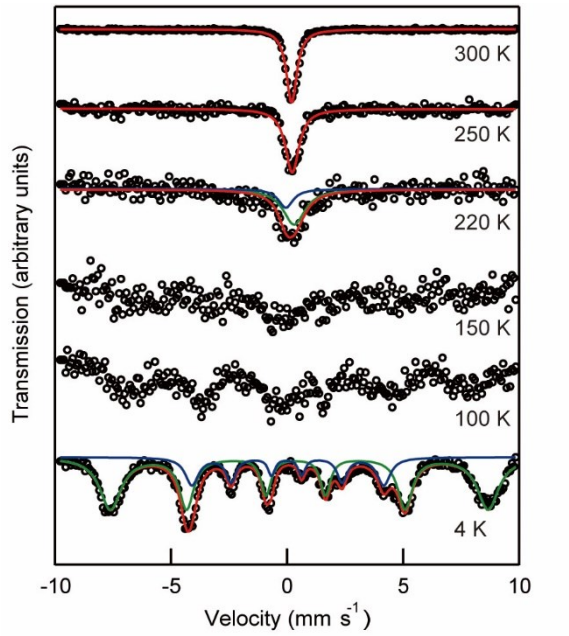

Figure S2. Mössbauer spectrum measured at different temperatures. The black cycles indicate the counts and the solid lines respectively represent fit sum (red), green (Fe^{3+}) and blue (Fe^{5+}).

Table SI. Refined structure parameters for $Sr_{0.5}La_{0.5}FeO_3$ against room temperature SXRD data. In the structure refinement the rhombohedral crystal structure was analyzed with the hexagonal cell. The cation (M)-O bond lengths calculated for the refinement result and the BVS are also listed.

Atom	Site	*x*	*y*	*z*	U_{iso}	Occupancy	BVS
Sr	6*a*	0	0	0.25	0.0029(7)	0.48 (1)	2.3
La	6*a*	0	0	0.25	0.0029(7)	0.51 (-)	2.5
Fe	6*b*	0	0	0	0.0007(9)	1.0	3.5
O	18*e*	0.534(2)	0	0.25	0.004(2)	1.0	-

Space group: *R*–3*c*. *a* = 5.50701 (8) Å, *c* = 13.4086 (3) Å, and R_{wp} = 2.4%.

Table SII. Mössbauer parameters for $Sr_{0.5}Bi_{0.5}FeO_3$ at 200 K.

Components	IS (mm/s)	Line Width (mm/s)	Area Ratio (%)
Fe^{3+}	0.31	0.57	74.2
Fe^{5+}	-0.05	0.38	25.8